Effects of Payload Motions on the Nutational Stability of the Galileo Spacecraft

Guy K. Man* and Fidelis O. Eke†
Jet Propulsion Laboratory, California Institute of Technology, Pasadena, California

In the presence of spacecraft nutation, tracking of an inertially fixed target by the Galileo scan platform requires the use of two control loops to move the scan platform and the stator in such a way as to compensate for spacecraft motion. The effect of these control loops on spacecraft nutational stability is examined using an eigenvalue analysis approach as well as several computer analysis packages. It was found that the actions of these control loops tend to drive nutation to the point of neutralizing, and even overpowering, the damping actions of the spacecraft nutation damper for pointing directions close to the spacecraft's spin axis. Stable and unstable zones are mapped out for two sets of spacecraft mass properties and contributions of rotor asymmetry and stator flexibility are discussed.

Introduction

THE Galileo spacecraft is a dual-spin spacecraft designed for an interplanetary mission to Jupiter.[1] Its fully deployed configuration is shown in Fig. 1. It consists essentially of a rotor R carrying three long booms and a relatively flexible platform S, which will henceforth be referred to as the stator to distinguish it from the payload P called the scan platform and whose principal components are remote sensing cameras. The rotor is connected to the stator through a spin bearing assembly (SBA) that allows one degree of freedom of relative motion that is controlled by the "clock" control loop. Similarly, the scan actuator subassembly (SAS) links the scan platform to the stator and permits relative motion about an axis perpendicular to the rotor spin axis; this motion is governed by the "cone" control loop.

Nutation damping of the Galileo spacecraft is achieved passively through the pendulous motions of the rotor's longest boom, while the other two booms are used to adjust the rotor's balance in flight. Nutational stability would normally be guaranteed for Galileo by virtue of the fact that the ratio of the rotor spin inertia to the vehicle transverse inertia is far greater than one (≈ 1.4). However, because the nominal rotor spin axis is not a principal axis for the despun section, the clock control loop will interact with vehicle global motion.[2,3] Neglecting wobble for the moment, one possible state of the Galileo spacecraft is that in which the rotor spins at a constant rate relative to the stator and the stator's attitude is fixed inertially, with the scan platform bore sight pointed to a fixed target in space. The system angular momentum vector is then parallel to the rotor spin axis. A transient disturbance could cause the spacecraft to nutate about the angular momentum vector and, if it is desired to keep the scan platform bore sight pointed to the same inertial target, then the clock and cone control loops go into action—they impart oscillatory motions at nutation frequency to the stator (in the clock) and to the scan platform (in the cone) so as to compensate for nutation. This process is referred to as spacecraft motion compensation. It is known[4,5] that these types of control actions affect the vehicle's nutational motion—they will drive or attenuate nutation depending on the mass properties and pointing direction.

The study undertaken here differs from previous work in that: 1) the axis of rotation of the Galileo's scan platform is not parallel to its spin axis; 2) the mass centers of the rotor, stator, and scan platform are not collinear; 3) the effects of a nonaxisymmetric rotor are examined; and 4) the effects of stator flexibility are also examined.

One of the goals of this study is to map out the stability regions that correspond to the current mass property values of the Galileo spacecraft. The emphasis here will be on examining the combined effect of the control loops and the spacecraft's nutation damper by superposition, and hence arrive at a clear prediction of the scan platform pointing directions that must be avoided if a given global nutation damping time constant is desired. Another goal of this study is to compare the impact of two given sets of stator mass properties on spacecraft nutational stability. Both sets are such that the mass center of the despun section (stator plus scan platform) lies on the spin axis; the only difference between them is that one set has a reduced value of the y-z product of inertia achieved by adding about 10 kg of ballast to the stator for improved balance. In the remaining part of this paper, the term "dynamically balanced stator" will be used to characterize this latter set, while "statically balanced stator" will refer to the former.

Equations of Motion

The spacecraft is modeled, as shown in Fig. 2, as a system of three rigid bodies (rotor, stator, and scan platform) with the mass centers of the rotor, despun section, and whole system all lying on the spin axis and the mass center for the scan platform lying on the scan actuator axis.

The equations of motion of the system can be obtained simply by expressing that the time derivative in an inertial reference frame of the angular momentum of the system (or parts thereof) is equal to the applied torque. If this is done for the system, rotor, and scan platform, the resulting equations in dyadic form are

$$\begin{aligned} &I^R\cdot(\omega+\dot{\Omega})+I^R\cdot(\omega\times\Omega)+(\omega+\Omega)\times I^R\cdot(\omega+\Omega)+I^S\cdot\dot{\omega}\\ &+\omega\times I^S\cdot\omega+I^P\cdot(\dot{\omega}+\beta)+I^P\cdot(\omega\times\dot{\beta})\\ &+(\omega+\dot{\beta})\times I^P\cdot(\omega+\dot{\beta})+m_R r_R\times(\omega\times r_R)+m_R r_R\\ &\times[\omega\times(\omega\times r_R)]+m_s r_s\\ &\times(\dot{\omega}\times r_S)+m_S r_S\times[\omega\times(\omega\times r_S)]+m_p r_p\times(\dot{\omega}\times r_p)\\ &+m_p r_p\times[\omega\times(\omega\times r_p)]=0 \end{aligned} \tag{1}$$

Presented as Paper 84-1992 at the AIAA/AAS Astrodynamics Conference, Seattle, WA, Aug. 20-22, 1984; submitted Sept. 21, 1984; revision received March 11, 1985.

*Technical Group Supervisor. Member AIAA.
†Member of Technical Staff. Member AIAA.

$$I^R\cdot(\dot\omega+\dot\Omega)+I^R\cdot(\omega\times\Omega)+(\omega+\Omega)\times I^R\cdot(\omega+\Omega)$$
$$+m_Rr_1\times(\dot\omega\times r_1)+m_Rr_1\times[\omega\times(\omega\times r_1)]$$
$$+m_Rr_1\times a_0=T_{\mathrm{SBA}} \tag{2}$$

$$I^P(\dot\omega+\dot\beta)+I^R\cdot(\omega+\dot\beta)+(\omega+\dot\beta)\times I^P\cdot(\omega+\dot\beta)$$
$$+m_Pr_2\times(\dot\omega\times r_2)+m_Pr_2\times[\omega\times(\omega\times r_2)]$$
$$+m_Pr_2\times a_{\mathrm{A}}=T_{\mathrm{SAS}} \tag{3}$$

where

I = an inertia dyadic
m = mass
ω = angular velocity of the stator
Ω = angular velocity of the rotor relative to the stator
β = rotation vector of the platform relative to the stator
$\dot\beta$ = the scan actuator articulation angle ($\dot\beta=0$ when ℓ points in the negative z direction in Fig. 2)
a_0 = acceleration of the point 0 on the spin axis with respect to which the angular momentum of the rotor is found (see Fig. 3)
a_A = acceleration of the point A on the SAS axis with respect to which the angular momentum of the platform is found (see Fig. 3)
T_{SBA} = spin bearing assembly torque
T_{SAS} = scan actuator torque
r = position vector (indicated by a subscript) as shown in Figs. 2 and 3
R,S,P = rotor, stator, and platform, respectively, used as super- or subscripts

Eigenvalue Analysis

The state of pure spin characterized by $\omega=\dot\beta=0$, $\Omega=$const, and arbitrary values of β and clock angle constitutes a solution of the above set of dynamical equations (1-3), provided that the spin axis is a rotor principal axis. Linearization of the equations of motion about the solution yields

$$I^R\cdot(\dot\omega+\dot\alpha)+I^R\cdot(\omega\times\Omega_0)+\omega\times I^R\cdot\Omega_0+\Omega_0\times I^R\cdot\omega+I^S\cdot\dot\omega$$
$$+I^P\cdot(\dot\omega+\dot\beta)+m_Rr_R\times(\dot\omega\times r_R)+m_Sr_S\times(\dot\omega\times r_S)$$
$$+m_Pr_P\times(\dot\omega\times r_P)=0 \tag{4}$$

where ω, $\dot\beta$, and $\dot\alpha$ are small and Ω_0 and β_0 constants. Under perfect tracking conditions, a unit vector ℓ aligned with the scan platform bore sight will have zero inertial motion; that is,

$$\dot\ell=(\omega+\beta)\times\ell=0 \tag{5}$$

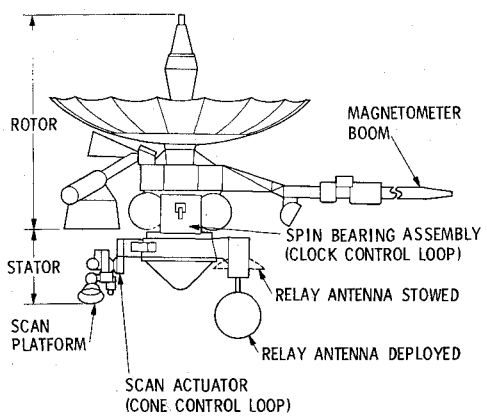

Fig. 1 Galileo spacecraft.

from which it follows that

$$\dot\beta=-\omega_y \tag{6}$$

$$\omega_z=\omega_x/\tan\beta_0 \tag{7}$$

and

$$\dot\omega_z\cong(\cot\beta_0)\dot\omega_x \tag{8}$$

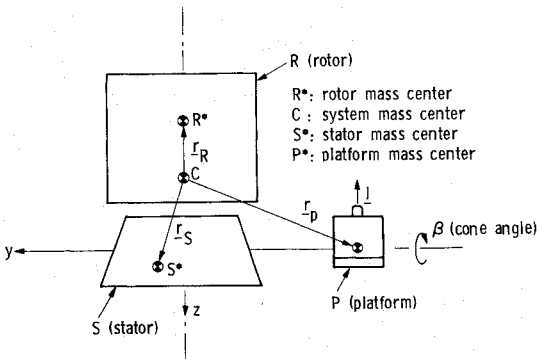

Fig. 2 Spacecraft model.

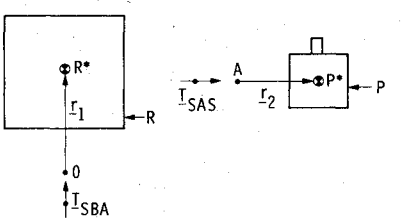

Fig. 3 Diagrams of rotor and platform.

Table 1 Mass properties

Parameter[a]	Statically balanced stator: Stowed relay antenna	Statically balanced stator: Deployed relay antenna	Dynamically balanced stator: Stowed relay antenna	Dynamically balanced stator: Deployed relay antenna
m_R, kg	809.20	809.20	809.20	809.20
m_S, kg	214.65	214.65	225.56	225.56
m_P, kg	81.32	81.32	81.32	81.32
I^R_{xx}, kg·m^2	2522.0	2522.0	2522.0	2522.0
I^R_{zz}, kg·m^2	4575.00	4585.00	4575.00	4575.00
I^S_{xx}, kg·m^2	165.90	176.90	188.60	200.50
I^S_{xy}, kg·m^2	−12.34	−11.07	−13.31	−11.98
I^S_{xz}, kg·m^2	−2.13	−4.13	−3.01	−5.02
I^S_{yy}, kg·m^2	56.26	65.38	57.58	66.61
I^S_{yz}, kg·m^2	−23.19	−27.08	−28.84	−32.87
I^S_{zz}, kg·m^2	160.40	157.60	180.50	177.70
I^P_{xx}, kg·m^2	4.90	4.90	4.90	4.90
I^P_{yz}, kg·m^2	0.18	0.18	0.18	0.18
r_x, m	0.	0.	0.	0.
r_{Ry}, m	0.	0.	0.	0.
r_{Rz}, m	−0.909	−0.909	−0.909	−0.909
r_{Sx}, m	0.	0.	0.	0.
R_{Sy}, m	0.535	0.535	0.509	0.509
r_{Sz}, m	0.351	0.378	0.359	0.385
r_{Px}, m	0.	0.	0.	0.
r_{Py}, m	−1.412	−1.412	−1.412	−1.412
r_{Py}, m	0.643	0.643	0.643	0.643

[a]Parameters not listed in this table are either not used explicitly in the equations or assume values of zero.

The control laws for realizing Eqs. (6) and (7) have been discussed in detail by Chodas and Man.[9] By substituting Eqs. (6-8) into Eq. (4), it becomes possible to isolate the two scalar equations governing the transverse rate of the stator and to put them in the form,

$$A\dot{\omega}_x + B\dot{\omega}_y + C\omega_y = 0 \tag{9}$$

$$D\dot{\omega}_x + E\dot{\omega}_y + F\omega_x = 0 \tag{10}$$

If it is assumed that the rotor is axisymmetric (i.e., $I_x^R = I_y^R = I^R$ and $I_{xy}^R = I_{xz}^R = I_{yz}^R = 0$), then the coefficients in Eqs. (9) and (10) are

$$\begin{aligned} A = {} & I^R + I_x^S + (I_{xz}^P + I_{xz}^S)\cot\beta_0 + I_z^P \\ & + m_R(r_{Ry}^2 + r_{Rz}^2 - r_{Rx}r_{Ry}\cot\beta_0) \\ & + m_S(r_{Sy}^2 + r_{Sz}^2 - r_{Sx}r_{Sz}\cot\beta_0) \\ & + m_P(r_{Py}^2 + r_{Pz}^2 - r_{Px} - r_{Pz}\cot\beta_0) \end{aligned} \tag{11}$$

$$B = I_{xy}^S - m_R r_{Rx} r_{Ry} - m_S r_{Sx} r_{Sy} - m_P r_{Px} r_{Py} \tag{12}$$

$$C = I_z^R \Omega_0 \tag{13}$$

$$\begin{aligned} D = {} & I_{xy}^S + I_{yz}^P \operatorname{cosec}\beta_0 + I_{yz}^S \cot\beta_0 - m_R(r_{Rx}r_{Ry} + r_{Ry}r_{Rz}\cot\beta_0) \\ & - m_S(r_{Sx}r_{Sy} + r_{Sy}r_{Sz}\cot\beta_0) - m_P(r_{Px}r_{Py} + r_{Py}r_{Pz}\cot\beta_0) \end{aligned} \tag{14}$$

$$E = I^R + I_y^S + m_R(r_{Rx}^2 + r_{Rz}^2) + m_S(r_{Sx}^2 + r_{Sz}^2) + m_P(r_{Px}^2 + r_{Pz}^2) \tag{15}$$

$$F = -I_z^R \Omega_0 \tag{16}$$

The negative reciprocal of the real part of the eigenvalues of Eqs. (9) and (10) is the nutation time constant t_C contributed by the clock and cone control loops. Hence,

$$t_C = 2(BD - AE)/(BF + DC) \tag{17}$$

A positive time constant implies nutation damping (stability) and a negative value indicates divergence of the nutation angle (instability).

Results

The nutation time constant due to the control loops, as given by Eq. (17), depends on the nominal cone angle β_0; Fig. 4 is a plot of t_C vs β_0 for a set of spacecraft mass properties corresponding to a statically balanced stator, zero tank fill, and no probe. The mass properties on which the results are based are summarized in Table 1. It is apparent that the clock and cone motions resulting from spacecraft motion compensation are destabilizing for $0 < \beta_0 < 90$ deg and $180 < \beta_0 < 270$ deg and stabilizing for $90 < \beta_0 < 180$ deg and $270 < \beta_0 < 360$ deg. The instability may be understood by re-examining Eq. (7). Any disturbance of the scan platform in a direction that is orthogonal to both the cone axis and the bore sight must rely on the clock control loop for compensation. This control effort will increase as the scan platform pointing direction moves toward the spin bearing axis ($\beta_0 \to 0$) because of the $1/\tan\beta_0$ factor that appears in Eq. (7). Thus, the energy generation rate of the clock control loop increases and, when it surpasses the energy dissipation rate of the passive nutation damper, spacecraft nutational instability results.

The combined effect of the nutation damper and the control loops on the nutational motion of the spacecraft can be represented in the form

$$1/t = 1/t_D + 1/t_C \tag{18}$$

where t_D is the nutation damper time constant, t_C the contribution of the control loops, and t the combined time constant. The Galileo nutation damper time constant in dual spin is known to remain below 5 min throughout the mission. Assigning then a worst case value of 5 min to t_D, the variation of t with β_0 is as shown in Figs. 5 and 6 for the four configurations under consideration. These figures may be used to map out the stable and unstable regions during spacecraft motion compensation. As an illustrative example, consider Fig. 5 and suppose that it is desired to keep the system nutation time constant below 10 min. A horizontal line corresponding to $t = 10$ min is drawn as shown in Fig. 5 and its intersections with the various segments of the graph indicate that t can be maintained below 10 min if the nominal cone angle β_0 is restricted as follows: $26 < \beta_0 < 180$ deg and $206 < \beta_0 < 360$ deg with the relay antenna stowed; $9 < \beta_0 < 180$ deg and $189 < \beta_0 < 360$ deg with the relay antenna deployed. Figures 7 and 8 summarize these and other results in the form of circle diagrams. These diagrams delineate three zones:

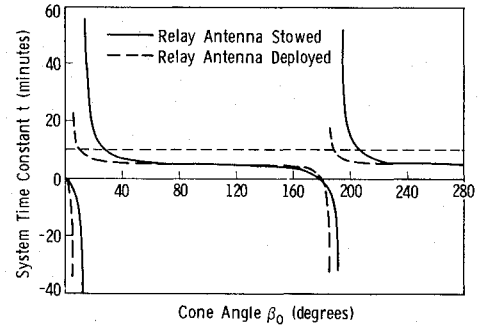

Fig. 5 Stability diagram for statically balanced stator, full tank empty, no probe.

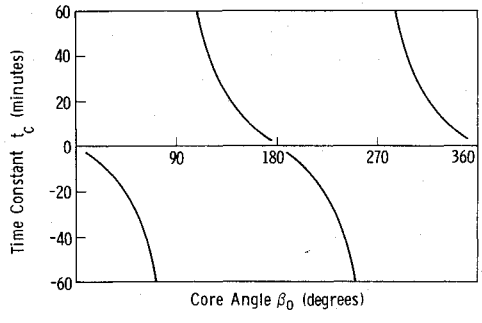

Fig. 4 Stability diagram for statically balanced stator, full tank empty, relay antenna stowed, no probe.

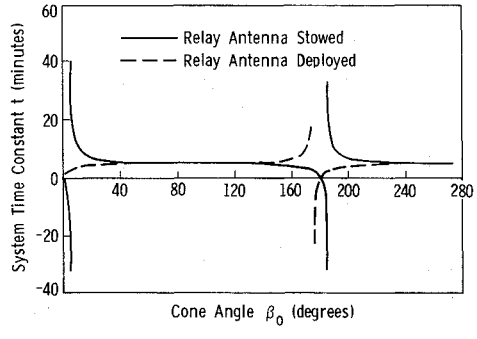

Fig. 6 Stability diagram for dynamically balanced stator, fuel tank empty, no probe.

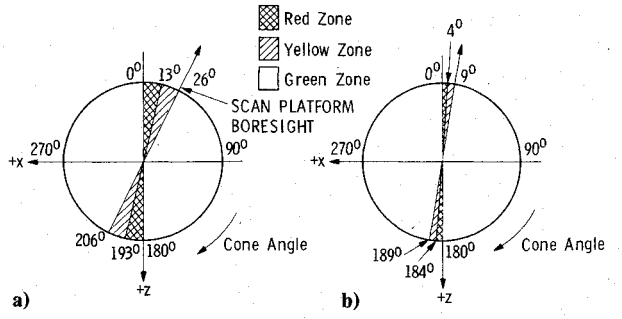

Fig. 7 Stability region for statically balanced stator: a) relay antenna stowed; b) relay antenna deployed.

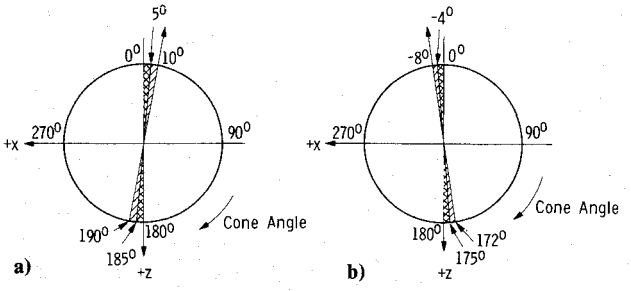

Fig. 8 Stability region for dynamically balanced stator: a) relay antenna stowed; b) relay antenna deployed.

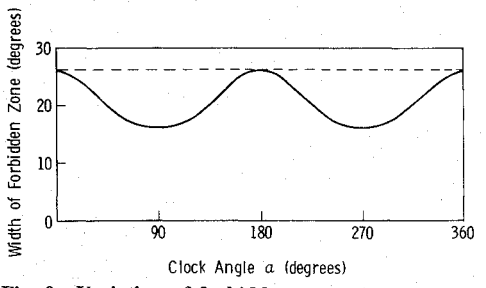

Fig. 9 Variation of forbidden zone with clock angle.

1) A zone of instability (red zone) in which the combined time constant is negative. Pointing in this zone will cause spacecraft nutation to grow with time.

2) A "yellow zone" in which the combined time constant is greater than the desired 10 min limit. Pointing in this region does not give rise to any instability; the only problem is that damping out a given nutation may take much longer than desired.

3) An "accessible" region (green zone) in which the combined time constant is positive and less than or at most equal to the assigned 10 min limit. This is the area to which all scan platform spacecraft motion compensation should be restricted.

The union of the red and yellow zones will henceforth be referred to as the "forbidden" zone.

One obvious fact shown by the circle diagram is that better dynamic balance decreases both the red and yellow regions. Note also that, in Fig. 8, deploying the relay antenna not only reduces these zones but also flips them over with respect to the z axis. This is due to a change in sign of the y-z product of inertia of the despun section when the antenna configuration changes from stowed to deployed. Similar circle diagrams can be drawn for any other value of the system time constant that one might choose. Changes in the desired system time constant affect all zones except the red one. For instance, increasing the limit on the system time constant shrinks the yellow region somewhat, but, as can be inferred from Figs. 5 and 6, the gain in the green region per unit rise in the system time constant limit decreases as the time constant limit is made higher.

The analysis presented was checked on a digital computer with the aid of symbolic manipulation software. The nonlinear equations of motion of the spacecraft excluding the nutation damper were obtained through the use of an automatic symbolic dynamical equations generation program SYMBOD.[6] The other analysis steps outlined in the section on the eigenvalue analysis were then carried out through the use of the symbolic manipulation program MACSYMA.[7] The equation for the time constant was transferred to a FORTRAN program where the hand-derived counterpart resided. The two equations were then compared numerically under a variety of spacecraft configuration conditions and showed identical results. These results were also spot checked by using the DISCOS[8] (dynamics interaction simulation of controls and structure) linear analysis package for an eigenanalysis of the system.

The use of symbolic manipulation software for this algebraic manipulation-intense analysis turned out to be invaluable in that the speed gained over the hand-derived method far outweighed the computer nuisance encountered (such as facility availability). It is estimated that, in general, once the system to be analyzed is defined, much time can be saved by using MACSYMA or similar tools to perform the algebraic manipulation of complex equations.

Asymmetry, Flexibility and Miscellaneous Considerations

The spin bearing angle did not play any role in the above results because the rotor was assumed to be axisymmetric, that is,

$$I_x^R = I_y^R$$

and

$$I_{xy}^R = I_{yz}^R = I_{xz}^R = 0$$

In reality, it is reasonable to assume $I_{yz}^R = I_{xz}^R = 0$ for Galileo because their nominal values are small and can be kept small via the spacecraft wobble control scheme. However, it is more difficult to justify $I_{xy}^R = 0$, unless, of course, one rotates the rotor-fixed system of axes about the spin axis to nullify I_{xy}^R. But, if this is done, then I_x^R ceases to be equal to I_y^R. Hence, more realistic results will be obtained either by keeping $I_x^R = I_y^R$ and making $I_{xy}^R \neq 0$ or by changing to another set of axes that gives $I_{xy}^R = 0$ but $I_x^R \neq I_y^R$. It turns out that the former option is easier to implement and leads to two new equations dependent on the nominal clock angle α_0 as well as β_0 in place of Eqs. (16) and (17), where α_0 is a constant. Stability results obtained from these new equations differ slightly from those obtained with the axisymmetry assumption. The widths of the red and yellow regions now vary with the clock angle. Figure 9 is a plot of the width of the forbidden zone vs the clock angle for zero tank fill and a dynamically balanced stator. It turns out that the curve obtained degenerates into the dotted straight line if the rotor is axisymmetric. Thus, for any given nominal clock angle, the area of the forbidden region corresponding to a nonaxisymmetric rotor is smaller than or at most equal to that corresponding to an axisymmetric rotor. Hence, the results in the previous section may safely be used as design criteria, since they actually represent a worst-case situation.

An attempt was made to examine the effect of stator flexibility on the contributions of the clock and cone loop to the global time constant of the system. This was done by using the DISCOS linear analysis package in which the rigid stator was replaced by a finite element model for which NASTRAN data were already available. This attempt quickly ran into difficulty because the composite inertia of the finite elements did not quite match the inertia values used for the rigid stator; and, since the stability analysis was very sensitive to changes in the stator mass properties, a meaningful comparison was impossible. Nevertheless, an assessment of the impact of flexiblilty was conducted by comparing results obtained from two

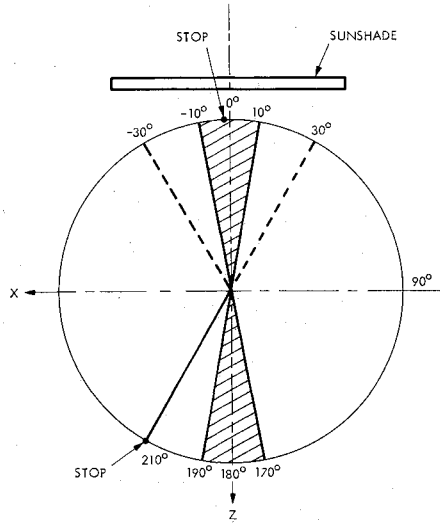

Fig. 10 Effective pointing zone.

DISCOS runs, both of which used the same finite element representation for the stator, except that flexiblity was suppressed in one of them by zeroing out all of the mode shape values. This time, the time constants were virtually identical and thus showed that flexibility effects were negligible.

Influence of tank fill and the probe were also examined, with the assumption that changes in tank fill affect only the mass properties. Tank fill was found to have no noticeable effect and keeping the probe on reduced the forbidden zone. Both these facts make sense intuitively since stator dynamic balance is the key issue here. If fuel (or oxidizer) depletion in opposite tanks proceeds at the same rate, there should be no change in spacecraft or stator balance and, hence, very little or no change in time constant. Furthermore, the probe is supposed to be axisymmetric, thus adding it to the stator (in the proper location) increases the mass of the despun section without contributing to the products of inertia, so that the dynamic imbalance per unit system mass is actually reduced. All the figures and diagrams presented in this paper are for zero tank fill and no probe; therefore, they represent worst-case situations.

Galileo scan platform control utilizes a number of methods for different control tasks.[9] The control method discussed thus far, defined by Eqs. (6) and (7), is called nonpolar region celestial pointing in the inertial mode. This is the prime control method for science. If the pointing direction of the scan platform is within 10 deg of the spin bearing axis, spacecraft motion compensation is suspended to avoid excessive torque demand by the control laws [Eqs. (6) and (7)]. This is referred to as polar region pointing. The control laws for pointing inside the polar region are

$$\dot{\beta} = -\omega_y \text{ and } \omega_z = 0 \tag{19}$$

The stability characteristics of the control system based on these control laws were examined by Breckenridge[10]; he found that the cone control is destabilizing when the scan platform mass center offset is greater than 5 cm or when I^P_{xy} is negative. This, however, is not a concern because the worst-case time constant of the control loop is in excess of 6 h.

The remaining control methods of concern are celestial pointing in cruise and stator pointing. They have identical control laws defined by

$$\dot{\beta} = 0 \text{ and } \omega_z = 0$$

The associated characteristic equation is neutrally stable and the time constant is infinite.

The above stability analysis assumes perfect pointing control laws. In reality, nonlinearities in the control loop, such as quantization effects and limited motor torques, prevent the control laws from being satisfied fully. Nevertheless, this analysis gives a conservative estimate of the stability region. For a system with high control gain, such as Gaileo platform pointing control, perfect control law assumption leads to excellent instability prediction for design purposes.

Summary and Recommendations

In the presence of spacecraft nutation, tracking of an inertially fixed target by the Galileo scan platform requires the use of the scan platform clock and cone control loops to move the platform and the stator in such a way as to compensate for spacecraft nutational motion. These actions of the control loops affect the global motion of the spacecraft: they amplify or attenuate nutation depending on the mass properties of the despun section, nominal pointing direction of the scan platform, and nutation damping time constant of the nutation damper. Unstable pointing regions have been found for the prime science pointing mode. If one assumes a time constant of 5 min for the Galileo nutation damper, then it is possible to keep the global nutation time constant at or below 10 min by avoiding any inertial pointing involving cone angles less than 26 deg measured in the positive direction from the poles. This value is for a statically balanced stator and can be reduced to 9 deg by keeping the relay antenna deployed during pointing. The corresponding values for a dynamically balanced stator (requiring an extra 10 kg of balast) are 10 and -8 deg, respectively.

The nutational stability problem of Galileo spacecraft carrying an inertial tracking scan platform has been described in detail in the previous section. The hazardous pointing regions have also been mapped out. Solution to this problem must be found to ensure safe spacecraft operation. Possible solutions are:

1) Detect excessive nutation and suspend scan platform spacecraft motion compensation control temporarily.

2) Impose operational limits on duration of spacecraft motion compensation activity in hazardous areas.

3) Expand the polar region where spacecraft motion compensation control is suspended to cover the "yellow" forbidden zone.

4) Optimize mass properties/configurations for greatest spacecraft motion compensation use.

It is felt that the first solution will lead to a pointing system that is unpredictable in performance and behavior, although it will give the widest possible pointing range. The second option is also undesirable in that operational constraints impose a burden on ground system. Onboard autonomy is preferred. The solution that is adopted by the Galileo spacecraft involves both solutions 3 and 4.

In the current flight software design, spacecraft motion compensation is disabled within 10 deg of the poles to avoid excessive torque demand. This zone is referred to as the polar region and is shown as shaded areas in Fig. 10. Moreover, the scan platform sunshade blocks the bore sight for cone angles of up to at least 30 deg on both sides of the zero line. Hence, the effective pointing region goes from about 30 to 170 deg, plus a small overtravel region between 190 and 210 deg. There are physical stops at 0 and 210 deg. By successively superimposing each of the diagrams of Figs. 7 and 8 onto Fig. 10, the following options for inertial pointing during spacecraft motion compensation emerge:

Option 1) One option is simply to use the statically balanced stator. The advantage of this option is the saving in mass of about 10 kg. The main disadvantage is the loss of practically the whole of the overtravel region. This does not constitute a real reduction in pointing capability, since this region is really redundant in the sense that any pointing that can be done inside it can also be done in its mirror image

relative to the 180 deg line, the only problem being that large clock slews and slew rates may sometimes be required. Finally, this option will require new flight rules or software changes to prevent an inadvertent request to perform inertial pointing with spacecraft motion compensation in the forbidden zones.

Option 2) A second option involves the use of a dynamically balanced stator. The main drawback here is the addition of 10 kg of dead mass with the attendant penalty in the form of increased propellant load or decreased tour length. Otherwise, this is a very good option because the whole of the forbidden region will then be contained inside the polar region and the effective pointing region is left intact. Also, no new flight rules or software changes need be established.

Option 3) A third possibility is to use the statically balanced stator and keep the relay antenna deployed during inertial pointing. The merits of this option include savings in mass and retention of the effective pointing region. However, an efficient way must be found to keep the antenna deployed at the right time.

Using a dynamically balanced stator with the antenna deployed is not a good option because nothing is gained by reducing the forbidden zone below 10 deg.

The third possibility seems to be the most attractive, combining most of the merits of the first two options and it is the option being adopted for actual implementation.

Current flight software is designed to suspend spacecraft motion compensation for scan platform pointing in the hazardous region defined in Fig. 7b. Since this is a small area, no real loss of useful pointing region resulted.

During the tour of the Jovian system, the relay antenna will always be deployed. However, ground sequence design must be constructed such that the relay antenna will be deployed at the right time during other portions of the mission for inertial pointing. This drawback turns out not to be a major problem because there are only a handful of times that inertial pointing of the scan platform will be exercised prior to arrival at Jupiter.

Conclusions

The Galileo dual-spin spacecraft can experience nutational instability if the scan platform is tracking an inertial target for certain pointing directions. The unstable pointing regions have been found and other effects such as rotor asymmetry and stator flexibility were examined. The solution adopted is to optimize the spacecraft balance by deploying a movable relay antenna during inertial target tracking and to suspend scan platform spacecraft motion compensation control when pointing in the hazardous areas.

Acknowledgment

The research described in this paper was carried out by the Jet Propulsion Laboratory, California Institute of Technology, under contract with the National Aeronautics and Space Administration.

References

[1]Yeates, C.M. and Clark, T.C., "The Galileo Mission to Jupiter," *Astronomy,* Vol. 10, Feb. 1982.

[2]Johnson, C.R., "TACSATI Nutation Dynamics," AIAA Paper 70-455, April 1970.

[3]Smay, J.W. and Slafer, L.I., "Dual-Spin Spacecraft Stabilization Using Nutation Feedback and Inertia Coupling," *Journal of Spacecraft and Rockets,* Vol. 13, Nov. 1976.

[4]McIntyre, J.E. and Gianelli, M.J., "The Effect of an Autotracking Antenna on the Nutational Stability of a Dual-Spin Spacecraft," AIAA Paper 72-571, April 1972.

[5]Farrenkopf R.L., "Stability of Dual-Spin Spacecraft Containing Tracking Payloads," AIAA Paper 72-890, Aug. 1972.

[6]Macala, G.A., "SYMBOD: A Computer Program for the Automatic Generation of Symbolic Equations of Motion for Systems of Hinge-Connected Rigid Bodies," AIAA Paper 83-0013, Jan. 1983.

[7]Bogen, K., et al., *MACSYMA Reference Manual,* The MATHLAB Group, Laboratory for Computer Science, Massachusetts Institute of Technology, Cambridge, Version Nine, Dec. 1977.

[8]Bodley, C.S., Devers, A.D., Park, A.C., and Frisch, H.P., "A Digital Computer Program for the Dynamic Interaction Simulation of Controls and Structures (DISCOS)," NASA TP 1219, May 1978.

[9]Chodas, J.L. and Man, G.K., "Design of the Galileo Scan Platform Control," *Journal of Guidance, Control and Dynamics,* Vol. 7, July 1984.

[10]Breckenridge, W.G., "Nutation Stability with Spacecraft Motion Compensation," Jet Propropulsion Laboratory, Pasadena, CA, Rept. IOM 343-82-348 (internal document), Apri 19, 1982.